

1
2 **Differential Motor System Entrainment to Auditory and Visual Rhythms**
3
4

5 Daniel C. Comstock^{1,2}, Ramesh Balasubramaniam²
6

7 ¹Center for Mind and Brain, University of California, Davis, CA, 95618, USA

8 ²Cognitive and Information Sciences, University of California, Merced, CA, 95343, USA
9

10
11 **Running Title:** Motor System Entrainment to Auditory and Visual Rhythms
12

13 **Keywords:** EEG, Entrainment, Rhythm Cognition, Mu Rhythms, Motor System
14
15
16

17 Address for Correspondence:
18

19 Daniel C. Comstock
20 Center for Mind and Brain
21 University of California, Davis
22 267 Cousteau Pl, Davis, CA 95618
23 Ph: 530.754.4526
24 dccomstock@ucdavis.edu
25
26
27
28
29
30
31
32
33
34
35
36
37
38
39
40
41
42
43
44
45
46

47 **Abstract**

48 Perception of, and synchronization to, auditory rhythms is known to be more accurate
49 than with flashing visual rhythms. The motor system is known to play a role in the processing of
50 timing information for auditory rhythm perception, but it is unclear if the motor system plays the
51 same role for visual rhythm perception. One demonstrated component of auditory rhythm
52 perception is neural entrainment at the frequency of the auditory rhythm. In this study we use
53 EEG to measure entrainment of both auditory and visual rhythms from the motor cortex while
54 subjects either tapped in synchrony with, or passively attended the presented rhythms. In order to
55 isolate activity from motor cortex, we used independent components analysis to first separate out
56 neural sources, then selected components using a combination of component topography, dipole
57 location, mu activation, and beta modulation. This process took advantage of the fact that
58 tapping activity results in reduced mu power, and characteristic beta modulation, that helped
59 select motor components. Our findings suggest neural entrainment in motor components was
60 stronger for visual rhythms than auditory rhythms, and strongest during the tapping conditions
61 for both modalities. We also find mu power increased in response to both auditory and visual
62 rhythms. These findings indicate that the generally greater rhythm perception capabilities of the
63 auditory system over the visual system may not depend entirely on neural entrainment in the
64 motor system, but rather how the motor system is able to utilize the timing information made
65 available to it.

66
67
68

69 **New and Noteworthy**

70 We investigated neural entrainment in the motor system for both auditory and visual
71 isochronous rhythms using electroencephalogram. Counter to expectations, our findings suggest
72 stronger entrainment for visual rhythms compared to auditory rhythms. Motor system activity
73 was isolated with a novel procedure using independent components analysis as a means of blind
74 source separation, along with known markers of mu activity from the motor system to identify
75 motor components.

76
77
78
79
80
81
82
83
84
85
86
87
88
89
90
91
92

93 Introduction

94 Human capability for sensorimotor synchronization (SMS) to auditory rhythms has been
95 shown to be more precise than SMS to visual rhythms (Repp, 2003), but the exact reasons why
96 are yet to be uncovered. It has been shown through fMRI work that activation of motor structures
97 are more pronounced for auditory rhythms than for visual rhythms during SMS tasks as (Hove et
98 al., 2013). This has led us to the suggestion that the auditory system is more tightly tied to the
99 motor system for temporal processing, such as needed for rhythm perception, than the visual
100 system which specializes in spatial processing. In previous works, we have suggested that a
101 corollary to this is that the visual system performs some rhythm processing in house (Comstock
102 & Balasubramaniam, 2018; Comstock et al; 2018; Comstock et al 2021). Based on that
103 suggestion, we would expect to see differences in electrophysiological measures of rhythm
104 processing in the motor system between auditory and visual rhythms that match those seen in
105 fMRI data.

106 The motor system plays a crucial role in the processing of music and auditory rhythms. A
107 meta-analysis on fMRI studies indicated activation of multiple regions of the motor system
108 during passive listening including right cerebellum, right primary motor cortex, and left and right
109 pre-motor cortices (Gordon et al., 2018). Other works have highlighted the importance of the
110 supplementary motor area (SMA) and basal ganglia in rhythm perception (Grahn & Brett, 2007;
111 Chen et al., 2008; Grahn & Rowe, 2009; Merchant et al., 2015). These structures are believed to
112 work in concert with the auditory system in order to drive the precise timing required in rhythm
113 perception. In their Action Simulation for Auditory Prediction (ASAP) hypothesis, Patel and
114 Iversen (2014) propose that this audio-motor facilitation is achieved through the dorsal auditory
115 stream. Likewise, Merchant and Honing (2014) also suggest a key role for the dorsal auditory
116 stream in rhythm processing in their Gradual Audiomotor Evolution (GAE) hypothesis, and also
117 highlight a central role for the motor cortico-basal ganglia thalamo-cortical circuit as a key
118 player in general timing processing. It is, however, not clear if there is a visuomotor equivalent
119 to the audiomotor coupling for the processing of auditory rhythms, or to what extent visual
120 rhythm timing is performed in the absence of motor system involvement. Further investigations
121 are needed to determine what role, if any, the motor system may play in visual rhythm
122 processing.

123 It has been demonstrated using EEG that listening to auditory rhythms elicits an increase
124 in power and phase coherence at the frequency of the beat of the rhythm (f_0), that is measured
125 most strongly over frontal-central regions (Nozaradan et al., 2011, 2012a, 2012b), and this signal
126 is increased during an SMS task (Nozaradan et al., 2015). Likewise, it has long been known that
127 the visual system can elicit power at the rhythm of visual flashes in what are dubbed steady-state
128 visually evoked potentials (SSVEPs) (for review see Vialatte et al., 2010). It is unclear to what
129 extent activity at f_0 induced for auditory rhythms and visual rhythms would both be present in
130 the motor system. If the auditory system is more tightly tied to the motor system than the visual
131 system however, we would expect measures of power and phase coherence in the motor system
132 to be stronger for auditory rhythms than visual rhythms.

133 Many previous EEG studies investigating activity from the motor system have attempted
134 to isolate motor system activity by selectively measuring activity from channels that lie over
135 motor regions (Pfurtscheller & Neuper, 1994; Pfurtscheller et al., 1997; McFarland et al., 2000).
136 One downside of this approach is that EEG activity arriving at the scalp level is a mix of all
137 sources of activity in the brain (Makeig et al., 2004). One method used to solve this issue is to
138 use independent components analysis (ICA), which has been shown to be an effective method of

139 separating out sources of neural activity in the brain (Delorme et al., 2012). While the blind
140 source separation of ICA allows for separating out sources, a method of selecting appropriate
141 sources for each study is required. Since this study aims to determine the role of the motor cortex
142 in rhythm processing, a clear marker of motor system activity will be needed.

143 One such marker can be found in Mu rhythms, which are a well-known marker of motor
144 system activity, and originate from the primary motor cortex in the range 8-13 Hz (Pfurtscheller
145 & Lopes da Silva 1999). Mu rhythms are known to reflect cortical idling and have been shown to
146 increase in power, or what is termed event-related synchronization (ERS), during movement
147 suppression, and decreased power or event-related desynchronization (ERD), during active
148 movements (Pfurtscheller & Neuper, 1994; Pfurtscheller et al., 1997; McFarland et al., 2000) as
149 well as during movement imagery (McFarland et al., 2000; Solomon et al., 2019). Isolating mu
150 activity using ICA based on component location and characteristics has been previously done in
151 research into the mirror neuron system (Nyström et al., 2011; McGarry et al., 2012; Behmer &
152 Fournier, 2016), and more recently to understand the role of mu in music perception (Ross et al.,
153 2022). Using a study design with a sufficient motor task, and a non-motor task could be expected
154 to induce modulation of mu rhythms that would make mu components further identifiable.

155 While previous work has primarily identified premotor and subcortical regions for
156 measuring rhythm processing, measuring activity generated from the primary motor cortex
157 through mu rhythm identified components is important as it is speculated that mu rhythms may
158 additionally serve as markers of rhythm perception, suggesting the primary motor cortex is
159 playing an additional role in processing rhythms. In previous work Ross et al., (2022) showed
160 that listening to music while remaining still results in mu ERS relative to silence. That study was
161 motivated by the premise in the ASAP hypothesis that the motor system is simulating the beat in
162 music (Patel & Iversen, 2014). While it remains unclear if beat simulation reflects covert motor
163 imagery of movement plans to a beat, or of a more abstract simulation of the beat in time, the
164 result is the motor system is able to send temporal predictions to the auditory system, as has been
165 measured through modulation of beta power (Fujioka et al., 2012, 2015, Comstock et al., 2021).
166 The findings in Ross et al., (2022) are then somewhat surprising given the previously stated
167 findings that mu activity reflects cortical idling as opposed to inhibition. A possible explanation
168 follows from reports that hand-area mu ERS has also been reported during foot movements
169 (Pfurtscheller & Neuper, 1994; Pfurtscheller et al., 1997). It may be that mu ERS during music
170 listening reflects an interaction between holding the hand still, and cortical processing for
171 movement or movement imagery elsewhere in the motor system, such as beat simulation.

172 In this study we used EEG to measure changes in mu rhythms and activity at the beat
173 frequency (f_0) induced by attending to isochronous auditory or visual rhythms. Based on the idea
174 that the auditory system is more tightly connected to the motor system than the visual system for
175 temporal processing, and that listening to music induces mu ERS as a result of motor system beat
176 simulation, we hypothesized that mu ERS would be greater for auditory rhythms than visual
177 rhythms during non-tapping conditions. Additionally, we hypothesized that activity at f_0 , as
178 measured by power and phase coherence, would reflect auditory rhythms more strongly than
179 visual rhythms in the motor cortex.

180
181
182
183
184

185 **Materials and Methods**

186

187 *Participants*

188 21 subjects participated in the experiment (11 female, $M = 21.62$ years, $SD = 3.58$). Data
189 from 3 subjects were not used, 2 for computer error and 1 due to poor signal to noise ratio
190 resulting in no discernable motor components. 10 subjects reported have some musical training
191 ($M = 6.6$ years training, $SD = 3.21$). All subjects had typical hearing and typical or corrected
192 vision, and reported being right handed. This study was approved by the UC Merced Institutional
193 Review Board for Research Ethics and Human subjects, and was carried out in accordance with
194 the Declaration of Helsinki. All participants gave written informed consent prior to testing.

195

196 *Task*

197 Subjects were seated and fitted with a 32 electrode EEG cap, and were presented with 16
198 stimulus trains with each train consisting of 40 events. 8 of the trains were of auditory tones
199 (1000 Hz sine wave, 50 ms duration with 10 ms rise and 30 ms fall), and the other 8 being visual
200 flashes (light grey flash with 50 ms duration). For both tones and flashes the subjects faced a
201 black computer screen with a grey fixation cross at the center that remained visible during both
202 flashes and tones. All stimuli were presented with an inter-onset interval of 600 ms, resulting in
203 beat frequency (f_0) of 1.667 Hz. Subjects were either instructed to tap in synchrony to the tones
204 or flashes using their right index finger, or to attend to the stimuli while remaining motionless.
205 During recorded subjects were observed to ensure they remained motionless except for tapping
206 in the appropriate conditions. Tap times were not recorded. The resulting four groups of stimulus
207 trains (auditory tapping, auditory non-tapping, visual tapping, visual non-tapping) were
208 presented as separate blocks, with each block having stimuli from only one condition. The order
209 of the groups was randomized with the exception that the 2 groups from each modality were
210 always presented one after the other, and the tapping order was preserved across modalities, e.g.,
211 visual non-tapping, visual tapping, auditory non-tapping, auditory tapping. In order to ensure
212 subjects were actively attending the stimuli, subjects were presented with an additional short test-
213 stimulus train immediately following each stimulus train, and were asked to compare the tempos
214 of the stimulus train with the short test stimulus train. The test-stimulus train was always of the
215 same modality as the stimulus train it followed, with tempo that was either slightly slower or
216 faster than the preceding train was presented. After the test-stimulus train was presented, subjects
217 were tasked with reporting if the later train was faster or slower than the previous train.
218 Following the end of each test-stimulus train and the start of each new stimulus train, participants
219 had a short break of a minimum of a 6 seconds.

220

221 *EEG Processing*

222 EEG data were recorded using an ANT-Neuro 32 channel amplifier using an ANT-Neuro
223 32 electrode Waveguard with electrode locations following the 10-20 International system. EEG
224 data were processed using EEGLAB 2021 (Delorme & Makeig, 2004) and Matlab 2020b. Data
225 were first downsampled from 1024 to 256 Hz, then high pass filtered with passband edge at 1 Hz
226 and -6 dB cutoff at .5 Hz. Data were then pruned so only the stimulus trains and 5 seconds prior
227 to each stimulus train remained, after which the data were inspected and bad channels were
228 removed. Spherical interpolation was used to fill the removed channels, after which ASR
229 correction was used to fix noisy bursts in single channels. Data were then referenced to average
230 and ICA was applied using the AMICA algorithm (Palmer et al., 2012). After ICA Dipoles were

231 fitted to the resulting components. Eye blink, eye movement, and heart artifact components were
232 selected by hand for each subject and removed from the data.

233 The independent components were then inspected using the IC Label toolbox (Pion-
234 Tonachini et al., 2019) to visualize and help determine which component corresponded to the left
235 hemisphere primary motor cortex for each subject based on the following criteria: Scalp
236 topography and dipole location indication that the component source was in the left motor
237 cortex, evidence of mu ERS in the spectral power, evidence of mu ERS in the time series based
238 on the distinctive mu wave shape, mu modulation based on condition (mu ERD during tapping
239 conditions). Left primary motor cortex components were found for all but 1 subject, resulting in
240 18 subjects. An example of a motor component can be seen in figure 1, along with the scalp
241 topography of all selected motor components. Further confirmation of the veracity of the motor
242 components was made following the time-frequency calculations by inspecting and comparing
243 beta power modulation between the tapping and no tapping conditions, as beta band power
244 attenuation from the motor cortex is known to occur during movement onset (Pfurtscheller &
245 Lopes da Silva, 1999). In this experiment, movement onset is expected to occur just prior to
246 stimulus onset as participants move to tap in synchrony with stimulus. All selected motor
247 components followed the expected pattern of beta modulation: clear beta power attenuation prior
248 to stimulus onset followed by increased beta power after stimulus onset during tapping
249 conditions, but not for the non-tapping conditions.

250

251

Figure 1 about here

252

253 Three separate time-frequency calculations were performed on the processed component
254 data: an analysis to inspect beta power modulation, and an analysis to calculate phase coherence
255 in the lower frequencies. To calculate beta power modulation, the data were epoched into 3
256 second epochs centered on the stimulus onset. Single-trial time-frequency analysis was
257 performed on the resulting epochs using Morlet wavelets between 8 and 35 Hz with a constant
258 wavelet length of 500 ms achieved using 4 cycles at 8 Hz and scaling up to 17.5 cycles at 35 Hz.
259 A divisive baseline consisting of the entire epoch length for each condition was used to highlight
260 power modulation of each frequency. The resulting time-frequency activity was used solely to
261 confirm that the selected motor components did indeed correspond to motor activity.

262 A second time-frequency calculation was performed on the un-epoched trials using
263 Morlet wavelets between 1.066 and 14.066 Hz with a constant wavelet length of 6563 ms
264 seconds achieved using 7 cycles at 1.066 Hz and 92.31 cycles at 14.066 Hz. The frequencies
265 used were linearly spaced at 0.1 Hz intervals so that the beat frequency of 1.666 Hz could be
266 captured. No baseline was used so that power could be compared across all 4 conditions. Using
267 the un-epoched data allowed for a wider window, removing potential edge artifacts that can arise
268 from using a narrow window, and additionally allowed for better bandwidth resolution with a
269 resulting constant bandwidth for each frequency of .3 Hz. Intertrial Phase Coherence (ITC) was
270 calculated by extracting the phase angles from the time-frequency calculations and epoching
271 them centered on each stimulus (+/- 300 ms), in a similar manner as implemented by Doelling &
272 Poeppel (2015). ITC was then calculated as phase coherence across epochs for each condition at
273 each time-frequency point for each component. Average ITC at each frequency was then
274 calculated by averaging across time.

275 A third time-frequency calculation was performed to extract mu activity from the selected
276 components on the un-epoched trials using a fast Fourier transform between 7 and 30 Hz with a

277 window length of 2 seconds. A divisive baseline specific to each condition was used with the
278 period defined as the 5 seconds prior to the start of each stimulus-train. Mu activity used for
279 analysis was the average power between 8 and 13 Hz and taken from the onset of the second
280 stimulus in each train to the end of the stimulus train.

281 To extract amplitude, a discrete Fourier transform was applied to the un-epoched data
282 from start of the second stimulus in each stimulus train, to the end of the train, using the length
283 of the entire stimulus train as the window size resulting in a frequency resolution of 0.0439 Hz.
284 To extract amplitude induced by the beat frequency, signal power for the individual frequencies
285 were noise corrected by subtracting the average power of the neighboring frequencies (+ 0.088 to
286 0.132 Hz and - 0.088 and 0.132 Hz) in a similar fashion as used by Nozaradan et al (2011).

287 *Statistical Analysis*

289 Analyses were carried out on the selected motor components for mu power, f0 amplitude,
290 and ITC. Analyses were also carried out on grand average activity for f0 amplitude and ITC to
291 assess overall activity without location bias as a point of comparison to other existing works,
292 e.g., Nozaradan et al (2011, 2015), Doelling & Poeppel (2015). The grand averages were
293 calculated for each subject for each condition, and consisted of the averages of the measures of
294 all components, which is equivalent to the grand scalp-average. One sample t-tests were used to
295 investigate if average calculated mu activity significantly increased in response to the stimuli
296 compared to baseline for each condition. To test if the rhythms induced a significant neural
297 response at f0, one sample-tests were used for each condition on the grand averaged data and
298 motor component data to test if the noise-corrected amplitude at f0 was greater than zero. Since
299 ITC activity is effectively always greater than zero, paired-sampled t-tests were used to
300 investigate if the rhythms induced significant phase coherence. ITC for both selected motor
301 components and for the grand averaged data was tested against randomly sampled ITC activity at
302 frequencies not likely to contain f0 activity or from any of the harmonics. To correct for multiple
303 comparisons, FDR was used on all test results (Benjamini & Hochberg, 1995).

304 To compare changes in mu power, noise corrected f0 power and f0 ITC across the four
305 conditions, separate 2 by 2 repeated measures ANOVAs were used with within-subject factors
306 being modality (audition and vision), and tap condition (no tapping and tapping). All statistical
307 analyses were performed using Jamovi (Version 2.2; The jamovi project 2021) statistical
308 software.

311 **Results**

313 *Mu Power*

314 one sample t-tests of mu activation in response to stimuli revealed increased mu activity
315 compared to baseline for the visual non-tapping conditions ($M = 2.316$, $SD = 3.08$) $t(17) = 3.192$,
316 $p = 0.021$ and for the auditory no-tapping conditions ($M = 2.208$, $SD = 3.34$) $t(17) = 2.801$, $p =$
317 0.025 , but not for either tapping condition (figures 2 & 3)

319 Analysis of power for mu activity from left motor component data showed a main effect
320 only for tapping $F(1,17) = 13.072$, $p = 0.002$, $\eta_p^2 = 0.445$, indicating mu activity was greater
321 during non-tapping conditions ($M = 2.262$, $SE = 0.713$) than during tapping conditions ($M = -$
322 0.248 , $SE = 0.2.93$).

323
324
325
326
327
328
329
330
331
332
333
334
335
336
337
338
339
340
341
342
343
344
345
346
347
348
349
350
351
352
353
354
355
356
357
358
359
360
361
362
363
364
365
366
367
368

Figure 2 about here

Figure 3 about here

Beat induction at f0

Single-sample t-tests of amplitude at f0 indicated all conditions induced significant amplitude in the grand average conditions, and for both tapping conditions in the motor components (table 1a, 1b, figure 4). Amplitude in f0 for the visual non-tapping conditions near significant at $p = 0.059$ (table 1a). Paired-sample t-tests of ITC at f0 indicated all conditions induced significant phase-coherence for both grand averaged and left motor component data (table 1c, 1d, figure 5).

Table 1 about here

Amplitude at f0

The repeated measures ANOVA of amplitude at f0 for the grand averaged data show only a main effect for modality $F(1,17) = 8.439$, $p = 0.010$, $\eta_p^2 = 0.332$, indicating greater f0 amplitude for the visual modality ($M = 1.094$, $SE = 0.111$) than the auditory modality ($M = 0.65$, $SE = 0.091$) (figure 4 d). We report no interaction effects, and therefore no post-hoc tests. The repeated measures ANOVA of amplitude at f0 for the left motor component data shows only a main effect for tapping $F(1,17) = 17.346$, $p < 0.001$, $\eta_p^2 = 0.509$, indicating greater f0 amplitude in the tapping conditions ($M = 0.216$, $SE = 0.032$) than in the non-tapping conditions ($M = 0.053$, $SE = 0.03$) (figure 4b).

Figure 4 about here

Examination of the scalp topography of f0 power indicates power peaking in the frontal-central region for auditory conditions, with stronger activity for the auditory tapping condition than the auditory not-tapping condition. Similar activity in the topography is seen in the visual conditions except there is additional stronger activity peaking over the posterior regions that does not appear to change between tapping conditions. (figure 5)

Figure 5 about here

ITC

The repeated measures ANOVA of ITC on grand averaged data revealed main effects for modality $F(1,17) = 17.653$, $p < 0.001$, $\eta_p^2 = 0.509$, indicating visual ITC at f0 ($M = 0.364$, $SE = 0.014$) was greater than auditory ITC at f0 ($M = 0.311$, $SE = 0.009$). We additionally find a main effect for tapping $F(1,17) = 26.283$, $p < 0.001$, $\eta_p^2 = 0.607$, showing the tapping conditions ($M = 3.65$, $SE = 0.014$) had greater f0 ITC than the non-tapping conditions ($M = 0.31$, $SE = 0.007$) (figure 6 d). There were no interaction effects seen in the grand averaged f0 ITC. The repeated measures ANOVA of ITC on left motor components data revealed main effects for modality $F(1,17) = 11$, $p = 0.004$, $\eta_p^2 = 0.394$, and for tapping $F(1,17) = 19.961$, $p < 0.001$, $\eta_p^2 = 0.54$, with no interaction effects. The main effects result indicate left motor f0 ITC was greater in the visual conditions ($M = 0.481$, $SE = 0.032$) than in auditory conditions ($M = 0.359$, $SE = 0.031$),

369 and that left motor f0 ITC was greater in tapping conditions ($M = 0.525$, $SE = 0.041$) than in
370 non-tapping conditions ($M = 0.314$, $SE = 0.027$) (figure 6b).

371

372

373

Figure 6 about here

374

375 **Discussion**

376

377 *Summary of Results*

378 In this experiment, we compared the effects of synchronizing to, or passively attending,
379 auditory and visual rhythms on neural activations at the beat frequency and on mu rhythms. Our
380 results show clear activation of the beat frequency for both auditory and visual rhythms in the

381 motor system in ITC and in both ITC and noise-corrected power in grand averaged data,

382 suggesting both modalities can entrain rhythms at the beat frequency in neural populations

383 (figures 4 & 6). We additionally show strong differential activation at the beat frequency and in

384 mu power between tapping in synchrony to auditory and visual rhythms compared to passively

385 attending the rhythms, where tapping in synchrony increases both power (figure 4) and phase-

386 coherence (figure 6) at the beat frequency, while decreasing mu power (figures 2 & 3).

387 Surprisingly, we find evidence of stronger induced activation at the beat frequency from visual

388 rhythms over auditory rhythms in ITC measures (figure 6), yet see no evidence of differential

389 activation of mu rhythms nor of noise-corrected amplitude across modalities (figures 2, 3, & 4).

390 Inspections of the spectral topography plots of noise corrected amplitude for all components at f0

391 indicate that f0 amplitude is most modulated by tapping in the frontal-central regions for both

392 modalities, while both visual conditions show relatively high f0 power posteriorly (figure 5).

393 While we make no direct statistical comparisons between the activity from the left-motor

394 components and grand-averaged data, it does appear that amplitude at the beat frequency is seen

395 in the motor components clearly only when tapping, as opposed to in all cases in the grand

396 averaged data (figure 4). Yet when looking at ITC at f0, there appears to be stronger activation

397 for all conditions in the motor components compared to the grand averaged data (figure 6)

398 indicating stronger phase locking to the rhythms.

399

400 *Mu Power*

401 Mu rhythm activity is thought to increase during movement suppression (Pfurtscheller &

402 Neuper, 1994; Pfurtscheller et al., 1997), and has been shown that it can serve as a marker for

403 rhythmic timing processing (Ross et al., 2022), based on the idea that the motor system is

404 simulating the beat (Iversen & Patel, 2014; Ross et al., 2016), and that the work of beat

405 simulation may result in mu ERS. Existing work made it unclear if attending rhythms would

406 result in mu ERS or ERD as Wu et al., (2016) reported mu ERD while listening to music while

407 Ross et al., (2022) reported mu ERS. Our results are in line with those reported by Ross et al

408 (2022) where they showed mu ERS during music listening compared to baseline. We show mu

409 ERS in response to both auditory and visual rhythms, suggesting a modality general response to

410 rhythms at the level of the motor cortex. The effect found by Wu et al., (2016) may be due to

411 motor imagery, as the ERD was seen in trained pianists while they listened to piano pieces they

412 were familiar with, and therefore may have been imagining the movements required to play the

413 pieces. As the study did not test non-musicians, nor musicians with music they were not familiar

414 with, it cannot be confirmed that the mu ERD was a result of simply attending or processing of
415 music

416 It is well known that humans synchronize with greater precision and across a greater
417 range of tempi to auditory rhythms than to visual rhythms (see Repp & Su, 2013 for review).
418 One prominent explanation is that the auditory system is tightly tied into the motor system to use
419 the motor system for auditory rhythmic timing processing (Iversen & Patel, 2014; Ross et al.,
420 2016), while more recent work has suggested that the visual system is able to do some rhythmic
421 timing in house (Comstock & Balasubramaniam, 2018; Comstock et al., 2021). Under those
422 conditions, and given the assumptions that mu ERD is seen during motor imagery, it could be
423 expected that auditory rhythms would elicit mu greater ERD compared to visual rhythms if the
424 motor system is involved in beat simulation as stated in the ASAP hypothesis. Yet our results are
425 in line with Ross et al., (2022) showing mu ERS during the auditory rhythms, and we
426 surprisingly also show mu ERS during visual rhythms, with no significant differences between
427 the two.

428 These results can be interpreted in several ways. The simplest interpretation is as
429 evidence that the motor cortex is not simulating the beat for either auditory or visual rhythms.
430 However, we urge caution in interpreting the results in this way as mu ERS during the non-
431 tapping tasks may reflect an interaction between holding the hand still, and cortical processing
432 for movement or movement imagery elsewhere in the motor system, such as reported in the
433 interactions between hand-area mu during foot movements (Pfurtscheller & Neuper, 1994;
434 Pfurtscheller et al., 1997). This would suggest an unexpected result: the motor system is
435 engaging in rhythm processing equally for both auditory and visual rhythms. A further
436 explanation may be that the isochronous rhythms used in this study did not modulate mu activity
437 in the same way music would. This could be due to the isochronous rhythms simply not driving
438 motor beat simulation in a way that would differentiate between auditory and visual rhythms. A
439 final consideration on the mu results is that mu activity arising from the primary motor cortex is
440 known to be modulated by the premotor areas including SMA (Ulloa & Pineda, 2007). Given
441 that the SMA has been implicated in rhythm processing (Iversen & Patel, 2014; Merchant &
442 Honing, 2014; Ross et al., 2016), and since this study did not isolate pre-motor or SMA activity,
443 it may be pre-motor activity would show the differentiation we hypothesized between modalities.
444

445 *Activity at f_0*

446 Numerous studies have shown neural activation at the beat frequency of a rhythm in
447 power and phase coherence measures using a frequency tagging approach (Nozaradan et al.,
448 2011, 2012a, 2012b, 2015; Doelling & Poeppel, 2015). Likewise, visual rhythms have been long
449 known to entrain to flashing rhythms (Vialatte et al., 2010), although visual rhythms studies
450 usually look at activity at higher frequency ranges, e.g. 10 to 12 Hz, rather than at the lower
451 frequencies used for SMS or auditory rhythm perception tasks. A recent study (Varlet et al 2020)
452 has shown that audio-visual rhythms can elicit beta-coherence between EMG activity from a
453 subject's non-moving finger and EEG activity over the cortical motor region that was stronger
454 than elicited by audio rhythms alone, suggesting that information of the timing of the visual
455 rhythms is present in the motor system, even when the subject is instructed to remain motionless.
456 Counter to our hypothesis, the f_0 activity localized to the left motor cortex in the current study
457 revealed greater ITC for visual rhythms than auditory rhythms, although we find no modality
458 differences in the motor component data in mu activation or in noise-corrected f_0 amplitude.
459 This finding suggests that differences in SMS and rhythm perception capabilities between

460 auditory and visual rhythms may not be due to greater entrainment ability of one modality over
461 the other, but rather in how that entrained activity is utilized.

462 Recent findings have shown that synchronization to visual rhythms can be achieved with
463 similar levels of accuracy found in synchronization to auditory rhythms when those rhythms are
464 moving. Importantly, the rhythm must move in a compatible way to the synchronizing movement
465 (Hove et al., 2010; Varlet et al., 2014). Further improvements have been seen when the moving
466 visual rhythm follows an ecologically valid movement pattern, such as with a bouncing ball (Gan
467 et al., 2015; Iversen et al., 2015; Huang et al., 2018). Yet, the benefit of using moving visual
468 rhythms does not appear to apply when there is no explicit motor task (Silva & Castro, 2016; Gu
469 et al., 2020). When these findings are taken into consideration with the motor cortex f0 ITC
470 activity we report in response to visual rhythms, it suggests the visual system is tightly connected
471 to the motor system in a way that allows for precise timing in response to visual stimuli in the
472 same way the motor system can with auditory stimuli. However, that tight visuo-motor timing is
473 only facilitated when visual stimuli are action compatible. When the stimuli are not action
474 compatible, such as a flashing rhythm, or when there is no action intention, the motor system is
475 not able to facilitate the same level of timing precision as is seen in synchronizing to a bouncing
476 ball.

477
478

479 *Limitations and Future Directions*

480 One major limitation of this study is in its use of isochronous rhythms, and interpreting
481 the resultant frequency domain activity. There has been controversy over whether or not activity
482 at the beat frequency of a rhythm represents neural entrainment to a rhythm, or if the activity at
483 the beat frequency is essentially an artifact from applying an FFT to rhythmic stimulus to evoked
484 potentials (Capilla et al., 2011; Novembre & Iannetti, 2018; Rajendran & Schnupp, 2019). One
485 way around the issues is to use syncopated or metered stimuli that would produce little or no
486 increase in frequency power at the frequency of interest (Lenc et al., 2019, Nozaradan et al.,
487 2018). As this study was designed to use as simple stimuli as possible, one needs to take care to
488 not over interpret the results. Indeed, it is possible that greater f0 activity seen in visual rhythms
489 compared to auditory rhythms is simply due to the evoked potentials to visual stimuli being
490 generally more pronounced than those evoked from similar auditory stimuli. However, this
491 concern applies primarily only to the grand-averaged f0 ITC and noise-corrected power, as we
492 see it as unlikely that the activity measured from the components isolated in the left motor cortex
493 would contain large sensory evoked potentials, as those components are not sourced in either
494 auditory or visual regions.

495 Additionally, we cannot entirely rule out effects of possible attentional differences
496 between stimuli conditions. If the visual rhythms resulted in increased attentional focus
497 compared to the auditory rhythms, we may expect to see greater entrainment for visual
498 conditions. As we did not have a direct measure of attentional effort, nor did we inquire about
499 the participants level of effort, it is unclear if there were attentional differences between our
500 conditions.

501 A further limitation is taps were not recorded. Future studies of a similar design would be
502 able to directly connect SMS performance metrics with the neural data. This may be particularly
503 useful in understanding how musical expertise affects neural processing of rhythms. Further
504 explanations such as a role for error correction in driving auditory and visual rhythm processing
505 differences should be tested in future studies.

506
507
508
509
510
511
512
513
514
515
516
517
518
519
520
521
522
523
524
525
526
527
528
529
530
531
532
533
534
535
536
537
538
539
540
541
542
543
544
545
546
547
548
549
550
551

Conclusions

We showed that mu rhythm activity in response to passively attending and synchronizing to simple isochronous rhythms is not modulated by the modality of that rhythm. Further we find evidence that entrainment to visual rhythms may be stronger than auditory rhythms, even though humans are generally able to perceive and synchronize to auditory rhythms more precisely than to visual rhythms. This indicates that how the entrainment activity is utilized by the motor system is just as important as the entrainment activity itself. We suggest that how, and to what extent, the motor system is able to couple with the visual system for rhythm processing is dependent on the stimulus appropriateness and the action intention regarding that stimulus.

Acknowledgement

The work was supported by NSF grant BCS 1626505. A portion of this work was submitted in partial fulfillment of the dissertation of Daniel C Comstock.

Conflict of Interest

The authors do not have any conflicts of interest to declare.

Author Contributions

DCC and RB conceived and designed this study together. DCC ran all participants and conducted analyses. DCC and RB co-wrote the paper.

552 **References**

- 553
- 554 Bangert, M., & Altenmüller, E. O. (2003). Mapping perception to action in piano practice: a
555 longitudinal DC-EEG study. *BMC neuroscience*, *4*(1), 1-14.
- 556 Behmer Jr, L. P., & Fournier, L. R. (2016). Mirror neuron activation as a function of explicit
557 learning: changes in mu-event-related power after learning novel responses to ideomotor
558 compatible, partially compatible, and non-compatible stimuli. *European Journal of*
559 *Neuroscience*, *44*(10), 2774-2785.
- 560 Benjamini, Y., & Hochberg, Y. (1995). Controlling the false discovery rate: a practical and
561 powerful approach to multiple testing. *Journal of the Royal statistical society: series B*
562 *(Methodological)*, *57*(1), 289-300.
- 563 Capilla, A., Pazo-Alvarez, P., Darriba, A., Campo, P., & Gross, J. (2011). Steady-state visual
564 evoked potentials can be explained by temporal superposition of transient event-related
565 responses. *PloS one*, *6*(1), e14543.
- 566 Chen, J. L., Penhune, V. B., & Zatorre, R. J. (2008). Listening to musical rhythms recruits motor
567 regions of the brain. *Cerebral cortex*, *18*(12), 2844-2854.
- 568 Comstock, D.C. & Balasubramaniam, R. (2018). Neural responses to perturbations in visual
569 and auditory metronomes during sensorimotor synchronization.
570 *Neuropsychologia* <http://doi.org/10.1016/j.neuropsychologia.2018.05.013>.
- 571 Comstock, D. C., Hove, M. J., & Balasubramaniam, R. (2018). Sensorimotor synchronization
572 with auditory and visual modalities: behavioral and neural differences. *Frontiers in*
573 *computational neuroscience*, *12*, 53.
- 574 Comstock, D. C., Ross, J. M., & Balasubramaniam, R. (2021). Modality-specific frequency band
575 activity during neural entrainment to auditory and visual rhythms. *European Journal of*
576 *Neuroscience*, (in press)
- 577 Delorme, A., & Makeig, S. (2004). EEGLAB: an open source toolbox for analysis of single-trial
578 EEG dynamics including independent component analysis. *Journal of neuroscience*
579 *methods*, *134*(1), 9-21.
- 580 Delorme, A., Palmer, J., Onton, J., Oostenveld, R., & Makeig, S. (2012). Independent EEG
581 sources are dipolar. *PloS one*, *7*(2), e30135.
- 582 Doelling, K. B., & Poeppel, D. (2015). Cortical entrainment to music and its modulation by
583 expertise. *Proceedings of the National Academy of Sciences*, *112*(45), E6233-E6242.
- 584 Foxe, J. J., & Snyder, A. C. (2011). The role of alpha-band brain oscillations as a sensory
585 suppression mechanism during selective attention. *Frontiers in psychology*, *2*, 154.
- 586 Fujioka, T., Trainor, L. J., Large, E. W., & Ross, B. (2012). Internalized timing of isochronous
587 sounds is represented in neuromagnetic beta oscillations. *Journal of Neuroscience*, *32*(5),
588 1791-1802.
- 589 Fujioka, T., Ross, B., & Trainor, L. J. (2015). Beta-band oscillations represent auditory beat and
590 its metrical hierarchy in perception and imagery. *Journal of Neuroscience*, *35*(45),
591 15187-15198.
- 592 Gan, L., Huang, Y., Zhou, L., Qian, C., & Wu, X. (2015). Synchronization to a bouncing ball
593 with a realistic motion trajectory. *Scientific reports*, *5*(1), 1-9.
- 594 Gordon, C. L., Cobb, P. R., & Balasubramaniam, R. (2018). Recruitment of the motor system
595 during music listening: An ALE meta-analysis of fMRI data. *PloS one*, *13*(11),
596 e0207213.

597 Grahn, J. A., & Brett, M. (2007). Rhythm and beat perception in motor areas of the brain.
598 *Journal of cognitive neuroscience*, 19(5), 893-906.

599 Grahn, J. A., & Rowe, J. B. (2009). Feeling the beat: premotor and striatal interactions in
600 musicians and nonmusicians during beat perception. *Journal of Neuroscience*, 29(23),
601 7540-7548.

602 Gu, L., Huang, Y., & Wu, X. (2020). Advantage of audition over vision in a perceptual timing
603 task but not in a sensorimotor timing task. *Psychological Research*, 84(7), 2046-2056.

604 Hove, M. J., Fairhurst, M. T., Kotz, S. A., & Keller, P. E. (2013). Synchronizing with auditory
605 and visual rhythms: an fMRI assessment of modality differences and modality
606 appropriateness. *Neuroimage*, 67, 313-321.

607 Hove, M. J., Spivey, M. J., & Krumhansl, C. L. (2010). Compatibility of motion facilitates
608 visuomotor synchronization. *Journal of Experimental Psychology: Human Perception
609 and Performance*, 36(6), 1525.

610 Huang, Y., Gu, L., Yang, J., Zhong, S., & Wu, X. (2018). Relative contributions of the speed
611 characteristic and other possible ecological factors in synchronization to a visual beat
612 consisting of periodically moving stimuli. *Frontiers in Psychology*, 9, 1226.

613 Iversen, J. R., Patel, A. D., Nicodemus, B., & Emmorey, K. (2015). Synchronization to auditory
614 and visual rhythms in hearing and deaf individuals. *Cognition*, 134, 232-244.

615 Lenc, T., Keller, P. E., Varlet, M., & Nozaradan, S. (2019). Reply to Rajendran and Schnupp:
616 Frequency tagging is sensitive to the temporal structure of signals. *Proceedings of the
617 National Academy of Sciences*, 116(8), 2781-2782.

618 Makeig, S., Debener, S., Onton, J., & Delorme, A. (2004). Mining event-related brain
619 dynamics. *Trends in cognitive sciences*, 8(5), 204-210.

620 Merchant, H., Grahn, J., Trainor, L., Rohrmeier, M., & Fitch, W. T. (2015). Finding the beat: a
621 neural perspective across humans and non-human primates. *Philosophical Transactions
622 of the Royal Society B: Biological Sciences*, 370(1664), 20140093.

623 Merchant, H., & Honing, H. (2014). Are non-human primates capable of rhythmic entrainment?
624 Evidence for the gradual audiomotor evolution hypothesis. *Frontiers in neuroscience*, 7,
625 274.

626 McFarland, D. J., Miner, L. A., Vaughan, T. M., & Wolpaw, J. R. (2000). Mu and beta rhythm
627 topographies during motor imagery and actual movements. *Brain topography*, 12(3),
628 177-186.

629 McGarry, L. M., Russo, F. A., Schalles, M. D., & Pineda, J. A. (2012). Audio-visual facilitation
630 of the mu rhythm. *Experimental brain research*, 218(4), 527-538.

631 Niedermeyer, E. (1997). Alpha rhythms as physiological and abnormal phenomena.
632 *International Journal of Psychophysiology*, 26(1-3), 31-49.

633 Novembre, G., & Iannetti, G. D. (2018). Tagging the musical beat: Neural entrainment or event-
634 related potentials?. *Proceedings of the National Academy of Sciences*, 115(47), E11002-
635 E11003.

636 Nozaradan, S., Peretz, I., Missal, M., & Mouraux, A. (2011). Tagging the neuronal entrainment
637 to beat and meter. *Journal of Neuroscience*, 31(28), 10234-10240.

638 Nozaradan, S., Peretz, I., & Mouraux, A. (2012a). Selective neuronal entrainment to the beat and
639 meter embedded in a musical rhythm. *Journal of Neuroscience*, 32(49), 17572-17581.

640 Nozaradan, S., Peretz, I., & Mouraux, A. (2012b). Steady-state evoked potentials as an index of
641 multisensory temporal binding. *Neuroimage*, 60(1), 21-28.

642 Nozaradan, S., Zerouali, Y., Peretz, I., & Mouraux, A. (2015). Capturing with EEG the neural
643 entrainment and coupling underlying sensorimotor synchronization to the beat. *Cerebral*
644 *Cortex*, 25(3), 736-747.

645 Nozaradan, S., Keller, P. E., Rossion, B., & Mouraux, A. (2018). EEG frequency-tagging and
646 input–output comparison in rhythm perception. *Brain topography*, 31(2), 153-160.

647 Nyström, P., Ljunghammar, T., Rosander, K., & von Hofsten, C. (2011). Using mu rhythm
648 desynchronization to measure mirror neuron activity in infants. *Developmental science*,
649 14(2), 327-335.

650 Palmer, J. A., Kreutz-Delgado, K., & Makeig, S. (2012). AMICA: An adaptive mixture of
651 independent component analyzers with shared components. *Swartz Center for*
652 *Computational Neuroscience, University of California San Diego, Tech. Rep.*

653 Patel, A. D., & Iversen, J. R. (2014). The evolutionary neuroscience of musical beat perception:
654 the Action Simulation for Auditory Prediction (ASAP) hypothesis. *Frontiers in systems*
655 *neuroscience*, 8, 57.

656 Pion-Tonachini, L., Kreutz-Delgado, K., & Makeig, S. (2019). The ICLabel dataset of
657 electroencephalographic (EEG) independent component (IC) features. *Data in brief*, 25,
658 104101.

659 Pfurtscheller, G., & Da Silva, F. L. (1999). Event-related EEG/MEG synchronization and
660 desynchronization: basic principles. *Clinical neurophysiology*, 110(11), 1842-1857.

661 Pfurtscheller, G., & Neuper, C. (1994). Event-related synchronization of mu rhythm in the EEG
662 over the cortical hand area in man. *Neuroscience letters*, 174(1), 93-96.

663 Pfurtscheller, G., Neuper, C., Andrew, C., & Edlinger, G. (1997). Foot and hand area mu
664 rhythms. *International Journal of Psychophysiology*, 26(1-3), 121-135.

665 Rajendran, V. G., & Schnupp, J. W. (2019). Frequency tagging cannot measure neural tracking
666 of beat or meter. *Proceedings of the National Academy of Sciences*, 116(8), 2779-2780.

667 Repp, B. H. (2003). Rate limits in sensorimotor synchronization with auditory and visual
668 sequences: The synchronization threshold and the benefits and costs of interval
669 subdivision. *Journal of motor behavior*, 35(4), 355-370.

670 Repp, B. H., & Su, Y. H. (2013). Sensorimotor synchronization: a review of recent research
671 (2006–2012). *Psychonomic bulletin & review*, 20(3), 403-452.

672 Ross, J. M., Comstock, D. C., Iversen, J. R., Makeig, S., & Balasubramaniam, R. (2022).
673 Cortical mu rhythms during action and passive music listening. *Journal of*
674 *neurophysiology*, 127(1), 213-224.

675 Ross, J. M., Iversen, J. R., & Balasubramaniam, R. (2016b). Motor simulation theories of
676 musical beat perception. *Neurocase*, 22(6), 558-565.

677 Silva, S., & Castro, S. L. (2016). Moving stimuli facilitate synchronization but not temporal
678 perception. *Frontiers in Psychology*, 7, 1798.

679 Solomon, J. P., Kraeutner, S. N., Bardouille, T., & Boe, S. G. (2019). Probing the temporal
680 dynamics of movement inhibition in motor imagery. *Brain research*, 1720, 146310.

681 The jamovi project (2021). jamovi (Version 2.2) [Computer Software]. Retrieved from
682 <https://www.jamovi.org>

683 Ulloa, E. R., & Pineda, J. A. (2007). Recognition of point-light biological motion: mu rhythms
684 and mirror neuron activity. *Behavioural brain research*, 183(2), 188-194.

685 Varlet, M., Coey, C. A., Schmidt, R. C., Marin, L., Bardy, B. G., & Richardson, M. J. (2014).
686 Influence of stimulus velocity profile on rhythmic visuomotor coordination. *Journal of*
687 *Experimental Psychology: Human Perception and Performance*, 40(5), 1849.

688 Varlet, M., Nozaradan, S., Trainor, L., & Keller, P. E. (2020). Dynamic Modulation of Beta
689 Band Cortico-Muscular Coupling Induced by Audio–Visual Rhythms. *Cerebral Cortex*
690 *Communications*, 1(1), tgaa043.

691 Vialatte, F. B., Maurice, M., Dauwels, J., & Cichocki, A. (2010). Steady-state visually evoked
692 potentials: focus on essential paradigms and future perspectives. *Progress in*
693 *neurobiology*, 90(4), 418-438.

694 Wu, C. C., Hamm, J. P., Lim, V. K., & Kirk, I. J. (2016). Mu rhythm suppression demonstrates
695 action representation in pianists during passive listening of piano melodies. *Experimental*
696 *brain research*, 234(8), 2133-2139.

697
698
699
700
701
702
703
704
705
706
707
708
709
710
711
712
713
714
715
716
717
718
719
720
721
722
723
724
725
726
727
728
729
730
731
732
733

734 **Figure Legend**

735

736 **Figure 1**

737 Example of left motor component from a single subject. Characteristic mu wave shape can be seen in the time-series
738 data (a), which is present only during the non-tapping conditions (b). The topography of the component suggests its
739 source is from the left-motor cortex (c), while the spectral power shows the characteristic 10 Hz power with a beta
740 harmonic resultant from mu activity (d). Topographic plots of activity from the selected left motor components with
741 activity of all components averaged together can be seen in the top topographic plot (e). All individual left-motor
742 component plots from selected mu components are shown (f).

743

744 **Figure 2**

745 Average Event Related Spectral Perturbation (ERSP) plots from motor components for each condition showing time
746 frequency power response compared to rest (baseline period).. The dashed line at zero indicates stimulus train onset.
747 The area inside the dotted lines is the region of interest for mu activity.

748

749 **Figure 3**

750 Box pots depicting the distribution of power in the mu range (8 - 13 Hz) compared to baseline across conditions for
751 left-motor component activity. The center line of each box depicts the median the red circle indicates the mean.
752 ANOVA results indicate significant mu increase for both auditory and visual no tapping conditions, but no
753 difference across modalities.

754

755 **Figure 4**

756 Frequency domain representation of noise-corrected amplitude for left motor components (a) and grand average (c).
757 Average noise-corrected amplitude is represented with the dark blue line, and shaded areas represent 95%
758 confidence intervals. Box plots show distribution of noise-corrected amplitude at f0 for left motor components (b)
759 and grand average (d). The center line of each box depicts the median the red circle indicates the mean. ANOVA
760 results indicated greater f0 amplitude in visual conditions over auditory conditions in the grand averaged data (d)
761 and greater f0 amplitude in tapping conditions than non-tapping conditions in the left motor components (b).

762

763 **Figure 5**

764 Scalp topography of f0 amplitude from grand average data.

765

766 **Figure 6**

767 Frequency domain representation of ITC left motor components (a) and grand average (c). Subject average ITC is
768 represented with the thick red line, and individual ITC are shown in thin black lines.. Box plots show distribution of
769 ITC at f0 for left motor components (b) and grand average (d). The center line of each box depicts the median the
770 red circle indicates the mean. ANOVA results indicated both left motor component and grand average f0 ITC was
771 greater in visual conditions than auditory conditions and also greater in tapping conditions over non tapping
772 conditions.

773

774 **Table 1**

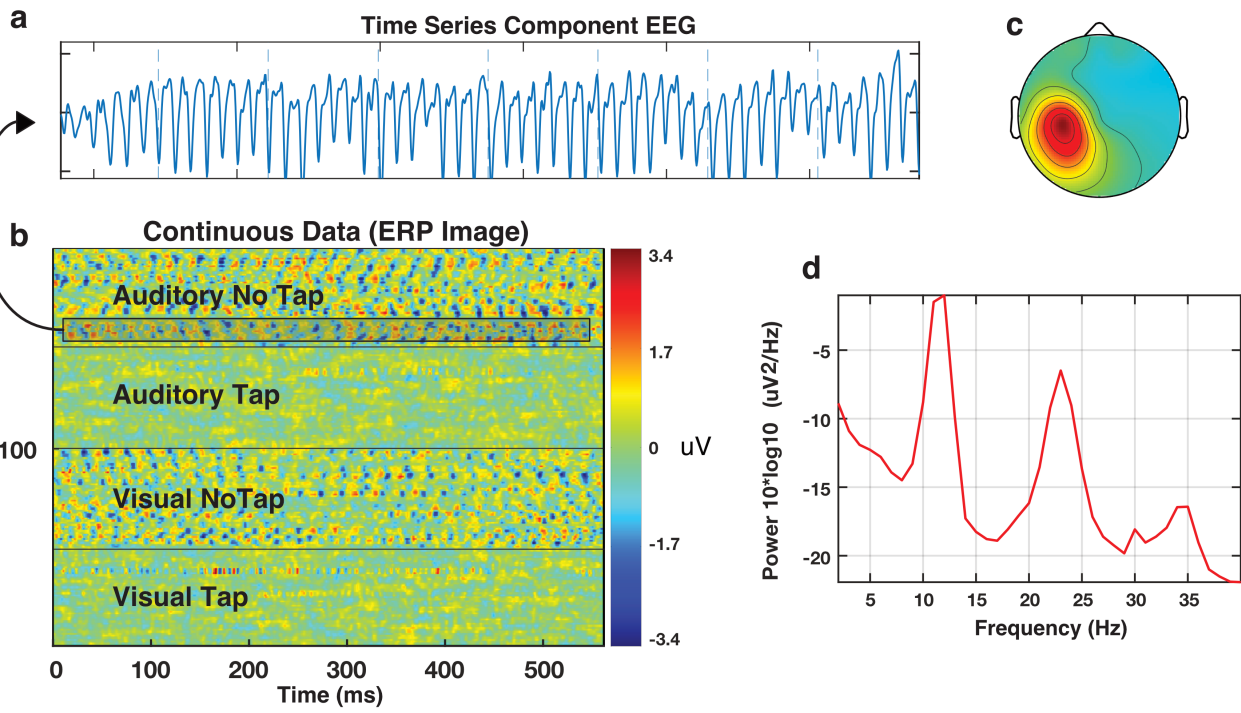
775 T-test tables for f0 amplitude and ITC. One-Sample t-test results comparing amplitude at f0 to zero for both motor
776 components (a) and grand average (b). Paired sample t-tests to assess if f0 ITC is significantly different from
777 randomly selected ITC values for both motor components (c) and grand average (d). Randomly sampled ITC values
778 are denoted as rSamp. All p-values are corrected for multiple comparisons using FDR correction.

779

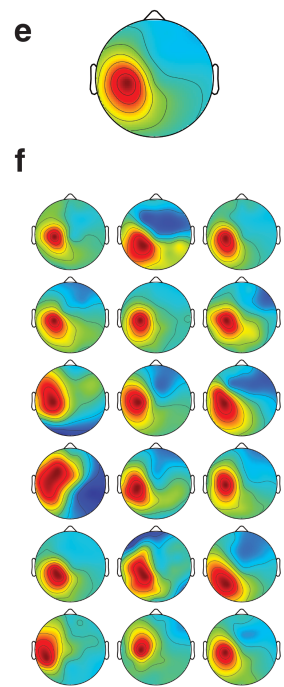
780

781

Left Motor component example

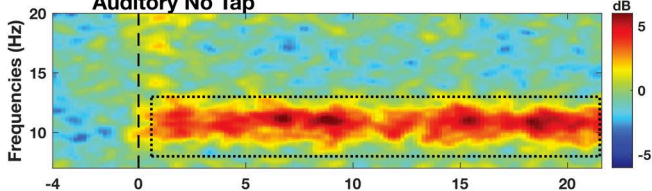


All Left Motor Components

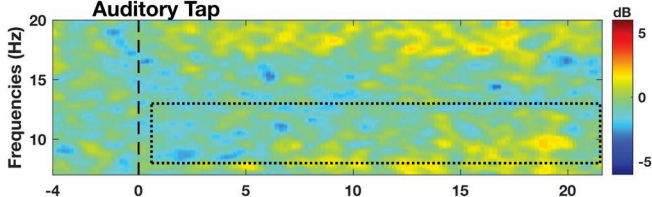


Left Motor Component ERSP

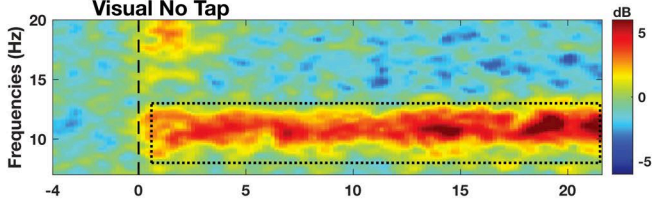
Auditory No Tap



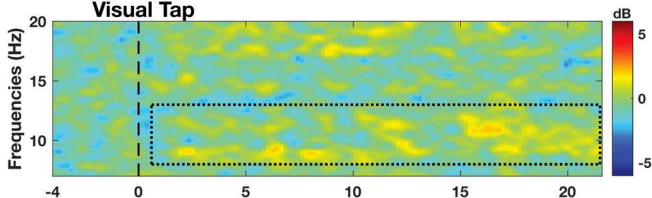
Auditory Tap



Visual No Tap

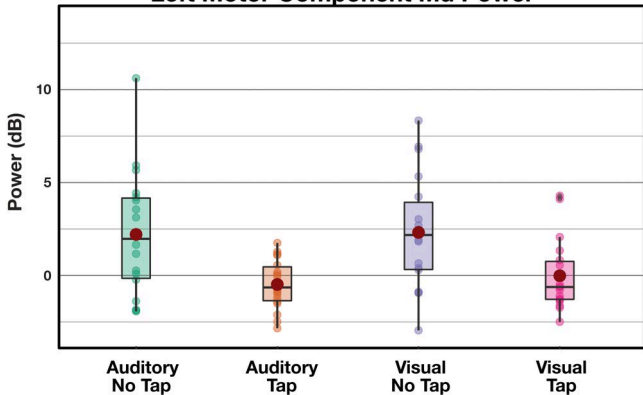


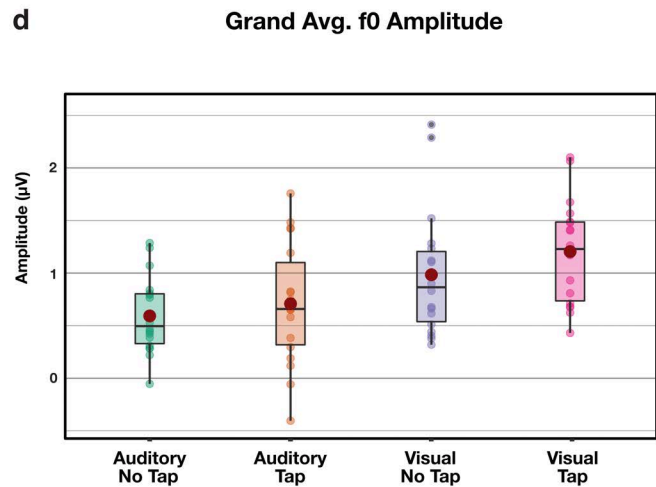
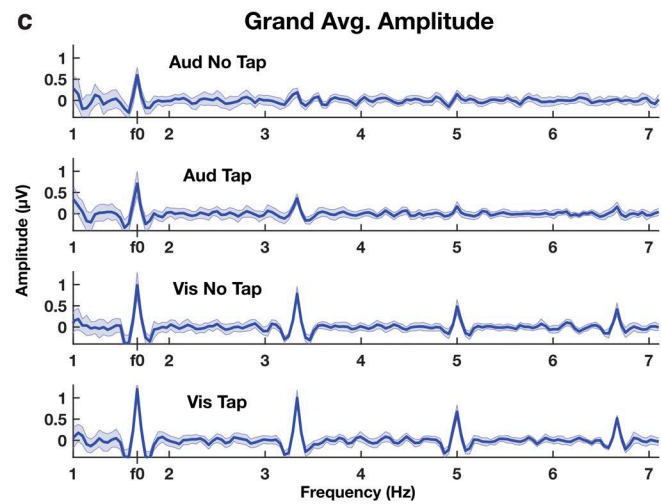
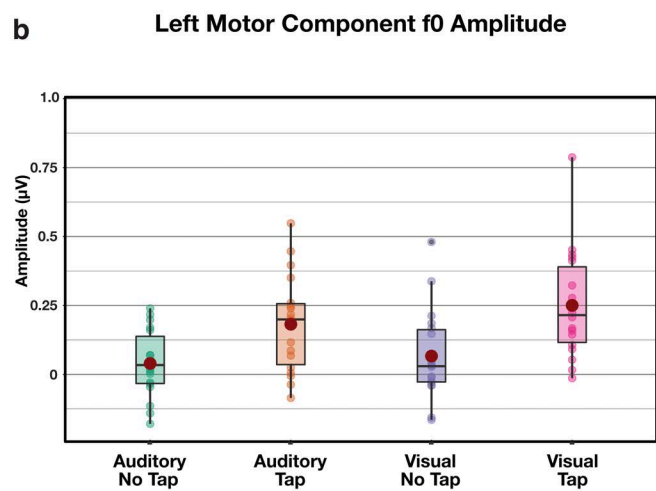
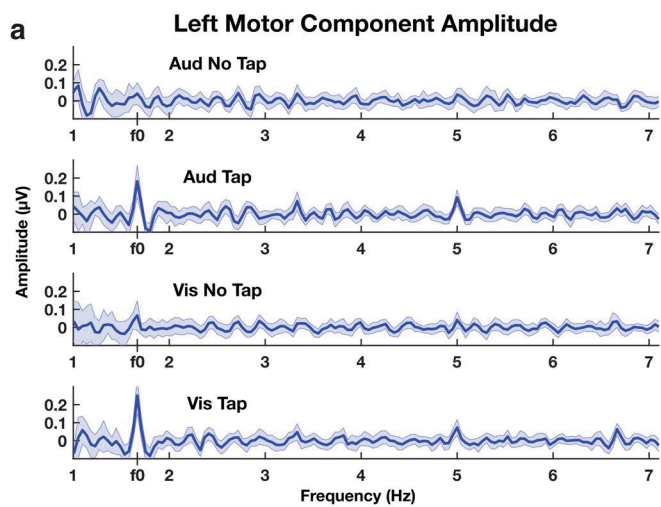
Visual Tap



Time (sec)

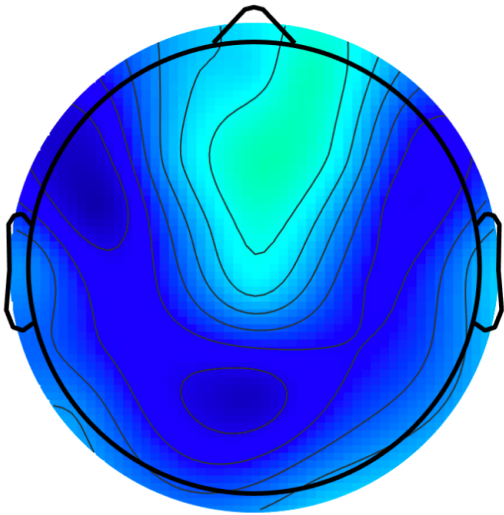
Left Motor Component Mu Power



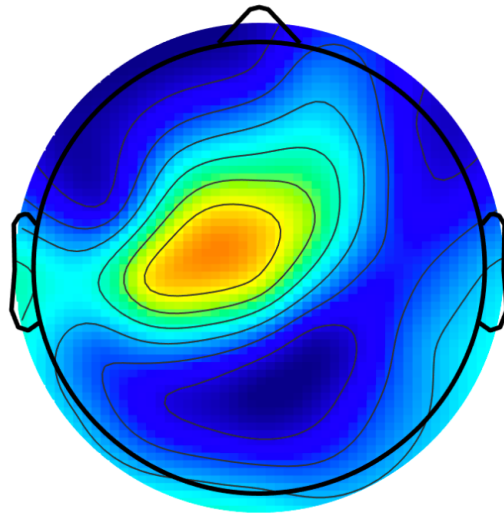


f0 Spectral Topography

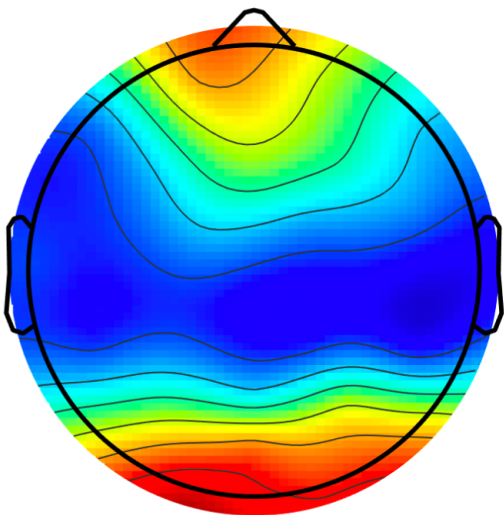
Aud No Tap (1.667 Hz)



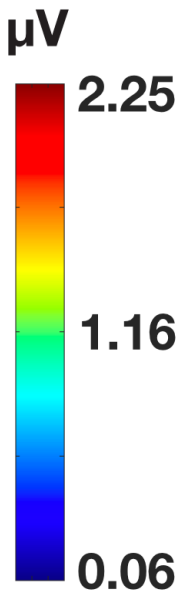
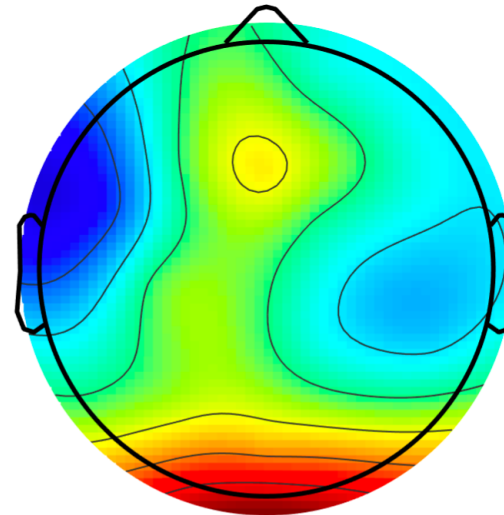
Aud Tap (1.667 Hz)

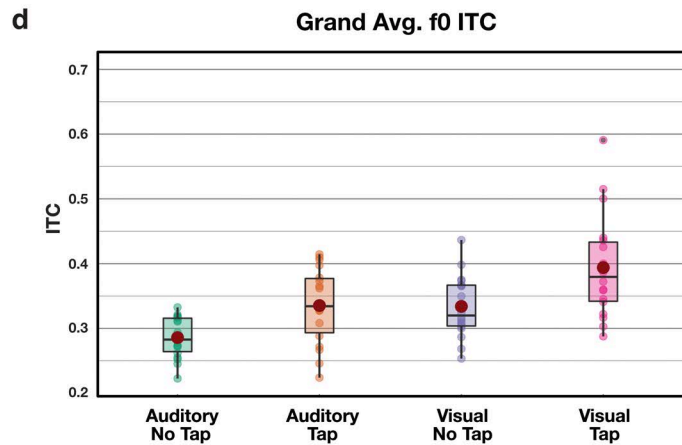
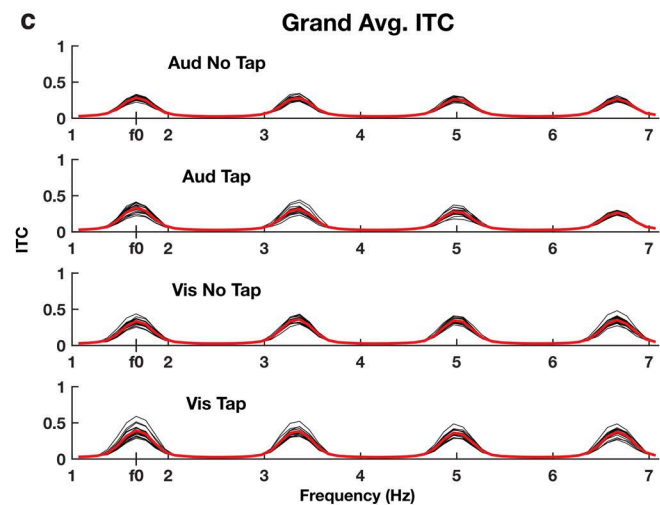
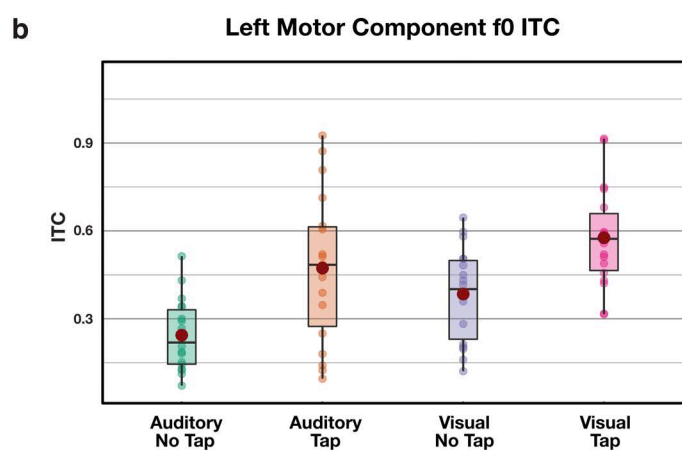
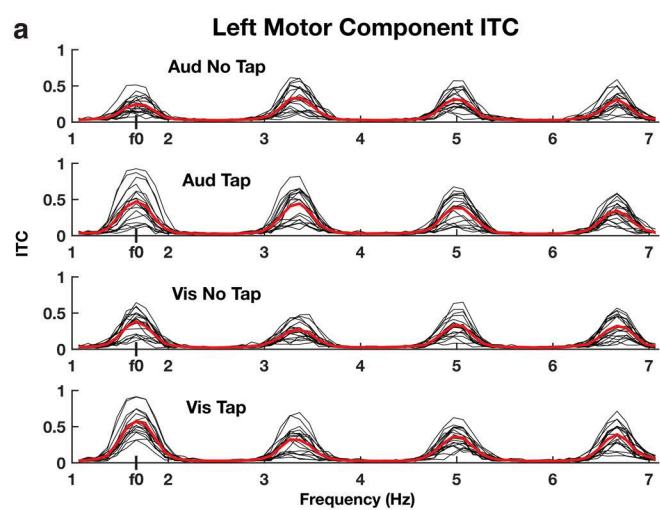


Vis No Tap (1.667 Hz)



Vis Tap (1.667 Hz)





Left Motor f0 Amplitude

One Sample T-Test

Condition	N	Mean	SD	t	df	p	Effect Size
L.Motor Aud No Tap	18	0.040	0.122	1.37	17	0.094	0.323
L.Motor Aud Tap	18	0.182	0.177	4.37	17	< .001	1.03
L.Motor Vis No Tap	18	0.066	0.164	1.72	17	0.059	0.405
L.Motor Vis Tap	18	0.250	0.198	5.37	17	< .001	1.267

Grand Avg. f0 Amplitude

One Sample T-Test

Condition	N	Mean	SD	t	df	p	Effect Size
Avg. Aud No Tap	18	0.593	0.364	6.92	17	< .001	1.63
Avg. Aud Tap	18	0.708	0.581	5.17	17	< .001	1.219
Avg. Vis No Tap	18	0.984	0.606	6.89	17	< .001	1.624
Avg. Vis Tap	18	1.204	0.492	10.39	17	< .001	2.45

Left Motor f0 ITC

Paired Samples T-Test

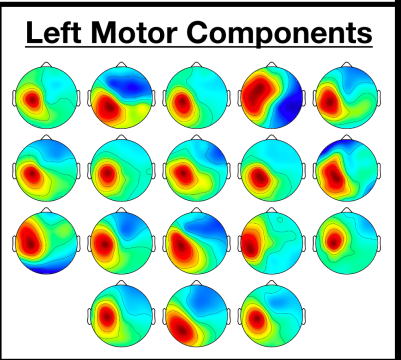
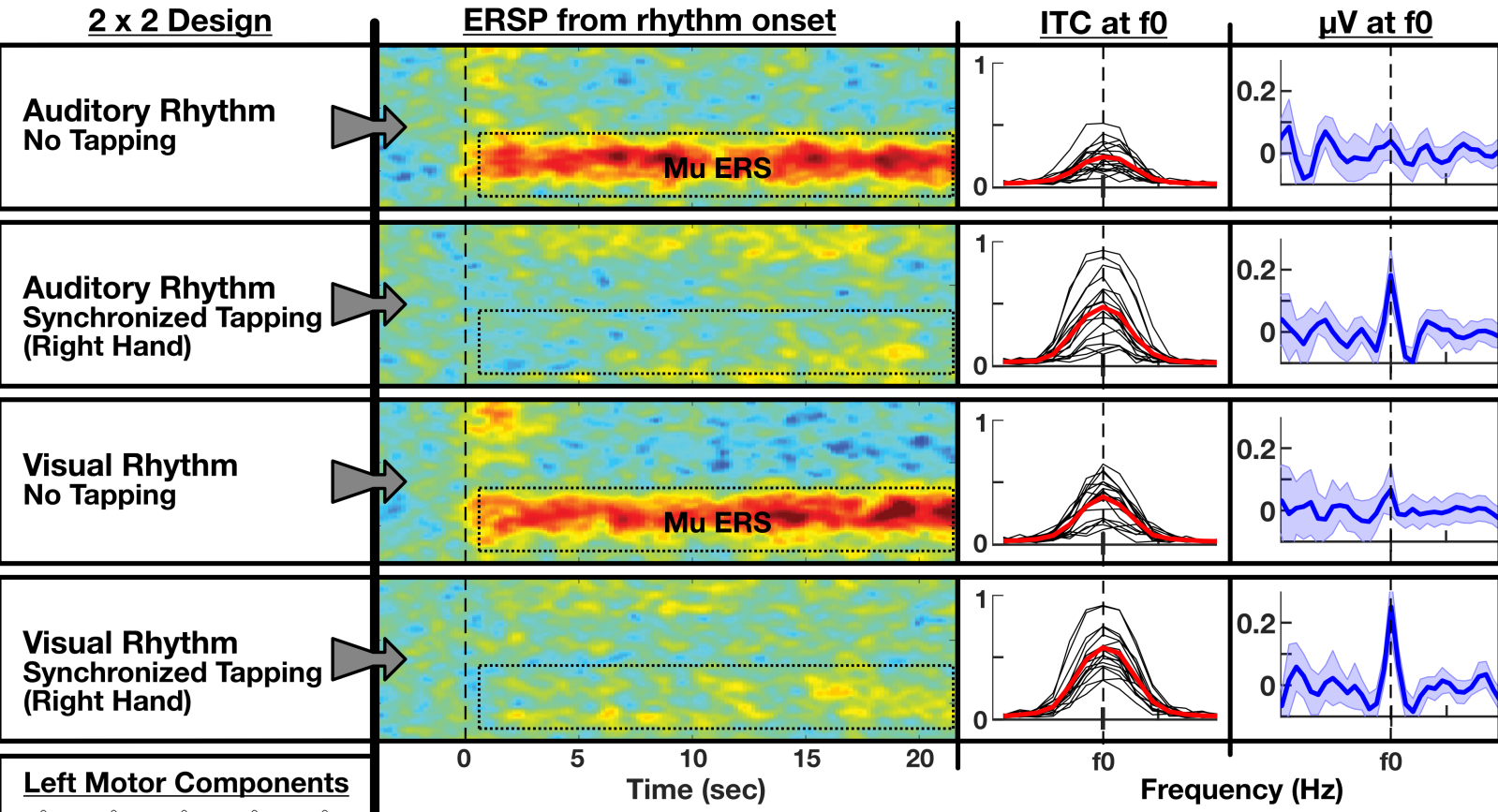
Condition	N	Mean	SD	t	df	p	Effect Size
L.Motor Aud No Tap	18	0.244	0.121	7.44	17	< .001	1.750
L.Motor Aud No Tap rSamp	18	0.031	0.003				
L.Motor Aud Tap	18	0.473	0.256	7.32	17	< .001	1.720
L.Motor Aud Tap rSamp	18	0.031	0.003				
L.Motor Vis No Tap	18	0.384	0.158	9.42	17	< .001	2.220
L.Motor Vis No Tap rSamp	18	0.030	0.004				
L.Motor Vis Tap	18	0.577	0.172	13.35	17	< .001	3.150
L.Motor Vis Tap rSamp	18	0.031	0.004				

Grand Avg. f0 ITC

Paired Samples T-Test

Condition	N	Mean	SD	t	df	p	Effect Size
Avg. Aud No Tap	18	0.286	0.031	34.15	17	< .001	8.050
Avg. Aud No Tap rSamp	18	0.031	0.002				
Avg. Aud Tap	18	0.335	0.058	22.16	17	< .001	5.220
Avg. Aud Tap rSamp	18	0.031	0.002				
Avg. Vis No Tap	18	0.334	0.048	27.08	17	< .001	6.380
Avg. Vis No Tap rSamp	18	0.031	0.002				
Avg. Vis Tap	18	0.394	0.080	19.30	17	< .001	4.550
Avg. Vis Tap rSamp	18	0.031	0.002				

Differential Motor System Entrainment to Auditory and Visual Rhythms



We investigated neural entrainment of motor cortex to auditory and flashing visual isochronous rhythms using ICA to isolate motor components. Both auditory and visual rhythms resulted in Mu ERS and significant phase coherence (ITC) at the beat frequency when subjects remained motionless. Visual ITC was stronger than auditory ITC, suggesting differential neural entrainment in motor cortex across modalities.